Liquid Crystals
Publication details, including instructions for authors and subscription information:
http://www.informaworld.com/smpp/title~content=t713926090

Electric field effects on the droplet structure in polymer dispersed cholesteric liquid crystals

H. -S. Kitzerow[ab]; P. P. Crooker[a]
[a] Department of Physics and Astronomy, University of Hawaii, Honolulu, Hawaii, U.S.A. [b] Iwan-N.-Stranski-Institut für Physikalische und Theoretische Chemie, Technische Universität Berlin, Berlin, Germany

To cite this Article Kitzerow, H. -S. and Crooker, P. P.(1993) 'Electric field effects on the droplet structure in polymer dispersed cholesteric liquid crystals', Liquid Crystals, 13: 1, 31 — 43
To link to this Article: DOI: 10.1080/02678299308029051
URL: http://dx.doi.org/10.1080/02678299308029051

LIQUID CRYSTALS, 1993, VOL. 13, NO. 1, 31–43

Electric field effects on the droplet structure in polymer dispersed cholesteric liquid crystals

by H.-S. KITZEROW†* and P. P. CROOKER
Department of Physics and Astronomy, University of Hawaii,
2505 Correa Road, Honolulu, Hawaii 96822, U.S.A.

(*Received 7 May 1992; accepted 24 July 1992*)

The behaviour of polymer dispersed cholesteric droplets in electric fields has been investigated for materials with both negative and positive dielectric anisotropy. Microscopic observations parallel and perpendicular to the electric field were performed. In materials with $\epsilon_a < 0$, the cholesteric pitch remains constant but a disclination ring occurs due to reorientation of the local helix directions. In systems with $\epsilon_a > 0$, however, helical unwinding was observed.

1. Introduction

Polymer dispersed liquid crystals (PDLC) are currently of high interest since nematic droplets dispersed in a polymer film can be used to produce large area flexible electrooptic displays [1, 2]. In such displays, randomly oriented nematic droplets cause diffuse scattering in the field-off state, while their uniform alignment by an electric field makes the film transparent because of refractive index matching. Recently, it has been shown that chiral nematic (cholesteric) [3] and chiral smectic [4] liquid crystals are also useful for PDLC display applications. In the cholesteric PDLC display [3] colour effects can be obtained using the selective reflection of highly chiral liquid crystals. In ferroelectric PDLC devices [4] the polymer film contains prealigned liquid crystal droplets; it behaves like a wave plate with tunable orientation of the optic axis so that the transmission between crossed polarizers can be modulated by electric fields.

In addition to technological applications, there is also interesting physics involved in the study of liquid crystal droplets. Here the director fields are complicated as a result of competition between: (1) elastic forces, which determine the director field for the liquid crystal in the bulk; (2) surface anchoring, which becomes dominant if the liquid crystal is confined to a very small cavity; and (3) field effects, which tend to align or disalign the director. In fact, cholesteric droplets in viscous fluids have attracted the interest of scientists for almost a century since the discovery of liquid crystals [5–10]. In most cases concentric fingerprint lines and a radial disclination line have been observed, revealing a modified cholesteric structure with planar surface anchoring and radial pitch axes, as suggested by Frank and Pryce [7, 8]. Recently, Yang and Crooker [11] have examined large cholesteric droplets (diameter $D \approx 50\,\mu m$) with large pitch ($p = 2$–$5\,\mu m$) as a model system to investigate the principles of their chiral PDLC display which utilizes small droplets ($D \approx 1$–$5\,\mu m$) of cholesteric materials with small

* Author for correspondence.
† Present address: Iwan-N.-Stranski-Institut für Physikalische und Theoretische Chemie, Technische Universität Berlin, D-1000 Berlin 12, Germany.

0267–8292/93 $10·00

pitch ($p = 300$–500 nm). Provided that the pitch is sufficiently large, polarization microscopy can be utilized to study in detail the effect of electric fields on the director configuration of the droplets.

Here, we report an investigation of large pitch cholesteric droplets of both positive and negative dielectric anisotropy. While previous observations [11, 12] have been made parallel to the field direction, we present for the first time observations of cholesteric droplets in which the direction of observation is perpendicular to the electric field. For negative dielectric anisotropy ($\epsilon_a < 0$) our results indicate the appearance of a disclination ring in the plane perpendicular to the field. The diameter of this ring increases continuously with increasing field strength, thereby changing the direction of the pitch axes while the pitch itself remains constant. For positive dielectric anisotropy ($\epsilon_a > 0$), on the other hand, we observe helical unwinding, i.e. the pitch increases with increasing field strength. We also report some preliminary observations of chiral droplets with perpendicular anchoring, which have director fields different from the well-known Frank–Pryce model. Finally, we summarize our various observations and classify the different structures in a way similar to the more extensively studied nematic droplet configurations.

2. Experiment

Each of the samples used in our experiments consisted of a liquid crystal mixture containing a chiral dopant and a nematic component with highly negative or positive dielectric anisotropy. Using the technique of temperature-induced phase separation [2], this liquid crystal mixture was dispersed in a thermoplastic polymer. For a liquid crystal with negative dielectric anisotropy ($\epsilon_a < 0$) and parallel anchoring at the droplet surface, we used the sample composition 2·9 wt% CE2 (BDH), 46·9 per cent ZLI 2806 (Merck), and 50·2 per cent PVB (Poly-(vinyl-butyral), Aldrich). For a liquid crystal with positive dielectric anisotropy ($\epsilon_a > 0$) and parallel anchoring, we investigated several samples with the approximate composition x per cent CB15 (BDH), (50-x) per cent E9 (BDH) and 50 per cent PMMA (Poly-(methyl-methacrylate), Aldrich). The concentration x of the chiral compound was varied up to 6·4 per cent to investigate the influence of the pitch on threshold voltages. To obtain negative dielectric anisotropy and perpendicular anchoring, we used 52·4 per cent PIBMA (Poly-(isobutyl-methacrylate), Aldrich) which is known to cause a radial structure for nematic droplets [1, 2], 1·8 per cent CE2, and 45·8 per cent EN18 (Chisso).

The respective liquid crystal and polymer were mixed at high temperature using chloroform as a solvent. After complete evaporation of the solvent, the homogeneous mixture was cooled slowly, causing phase separation of the liquid crystal and gelation of the polymer. A hot stage controlled by a PID pulse width thermostat (INSTEC) was used to control the temperature with an accuracy of $\pm 0{\cdot}01$°C. A constant cooling rate of 0·02°C min^{-1} resulted in droplet diameters of 10–40 μm, depending on the material.

The effect of electric fields on the cholesteric droplets was studied using a Zeiss Universal microscope, with samples placed between crossed polarizers and observed in transmission. In order to study the droplets either parallel or perpendicular to the field direction, two different cells were utilized. For observation parallel to the field, the sample was placed between ITO-coated glass plates separated by 31·2 μm glass spacers. The cells were prepared by placing the homogeneous mixture above the gelation temperature on one of the coated glass slides, completely evaporating the solvent, then covering the sample with a second ITO-coated glass slide and performing the slow cooling process described previously. For observation of the droplets perpendicular to

the field direction, however, the homogeneous mixture was placed between uncovered glass slides, with two parallel copper plates of 0·2 mm thickness used as both electrodes and spacers. A uniform distance of about 160 μm between the electrodes was achieved using glass spacers. Alternating voltages with a frequency of 1 kHz were applied to the samples; reported voltages are rms values.

3. Results

3.1. *Planar anchoring, no field*

For the cholesteric droplets dispersed in PVB and PMMA we observed concentric fingerprint rings and often a radial disclination line (see figure 1). This pattern is characteristic of the model proposed by Frank and Pryce [7, 8]. Like the bulk cholesteric phase, the director **n** is locally twisted along a pitch axis **q**(**r**), but the direction of **q** is everywhere radial. The phase relation between the helices along different directions results in a radial disclination line of strength $s=2$. If the disclination line is perpendicular to the viewing direction (see figure 1 (*a*)), it can be seen even without polarizers. However, if the disclination line is coincidentally oriented along the field direction it is not visible but the fingerprint lines form a spiral (see figure 1 (*b*)).

The textures represented in figure 1 were obtained by calculating the transmission of a light beam passing first through a polarizer, then through a cholesteric droplet described by the Frank–Pryce director field, and then through a second polarizer which is crossed with respect to the first. Details of this calculation, which uses the Müller–Stokes formalism [13] to calculate the effect of retardation and polarizer absorption, are given elsewhere [14]. For nematic droplets, our simulated textures are in agreement with the textures described in a paper by Ondris–Crawford *et al.* [15] who used Jones matrices [13] for their calculation. The result of our computation for cholesteric droplets confirms the agreement of the Frank–Pryce model with experimental observations [8].

3.2. *Planar anchoring, $\epsilon_a < 0$*

For liquid crystals with negative dielectric anisotropy it has been shown previously [11, 12] that application of an electric field leads to the appearance of a Grandjean texture in the centre of the droplet (see figure 2 (*a*)). However, previous observations, which were performed only along the field direction have not been sufficient to elucidate the exact topology of the field-induced director field. Our observations perpendicular to the field show that the concentric fingerprint rings become ellipse-like as the pitch axes attempt to align with the field. If the field exceeds a threshold value, the point at the centre of the rings evolves visually into a straight line with field-dependent length (see figures 2 (*b*) and (*c*)). Combining the results represented in figures 2 (*a*), (*b*) and (*c*), we conclude that the field causes the appearance of a disclination circle. Figure 3 shows the field dependence for the reduced radius of this circle for observations both parallel and perpendicular to the field. The two curves correspond to samples with different sample thicknesses and slightly different composition; nevertheless the functions are in good agreement. For the threshold field strength we have obtained the values $E_{\text{step},\parallel} = 0{\cdot}34\,\text{V}/\mu\text{m}$ and $E_{\text{step},\perp} = 0{\cdot}29\,\text{V}/\mu\text{m}$ for observation parallel and perpendicular to the field, respectively.

Although no theoretical model has yet been proposed for this behaviour, we have arbitrarily fitted the lines in figure 3 to the exponential growth function

$$r/R = 1 - \exp[(E - E_0)/E'].$$

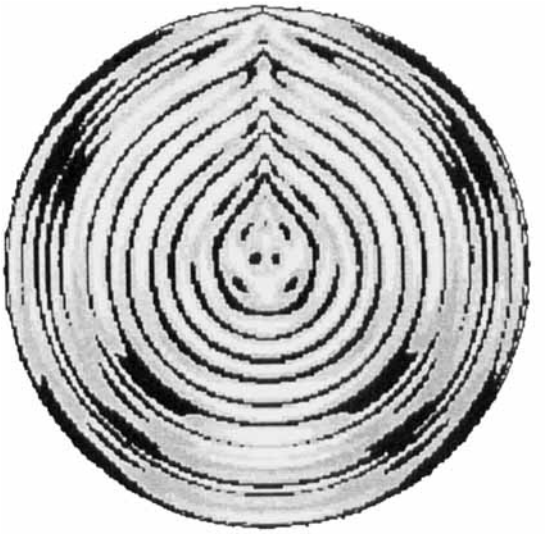

(*a*)

(*b*)

Figure 1. Calculated transmission of a cholesteric droplet between crossed polarizers. The director configuration corresponds to the Frank and Pryce model with: (*a*) disclination line perpendicular to the viewing direction (vertical), (*b*) disclination line parallel to the viewing direction.

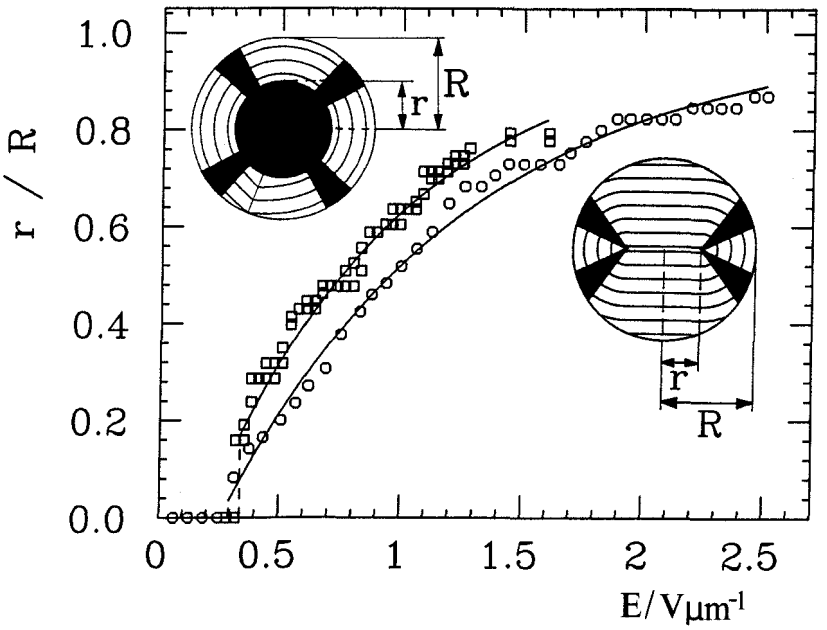

Figure 3. Reduced radius r of the disclination ring (R = radius of the droplet) versus field strength, determined from observation parallel (squares) and perpendicular (circles) to the field.

The fitting parameters are: $E_{0,\parallel} = 0{\cdot}19\ \mathrm{V}/\mu\mathrm{m}$, $E'_{\parallel} = 0{\cdot}82\ \mathrm{V}/\mu\mathrm{m}$, $E_{0,\perp} = 0{\cdot}26\ \mathrm{V}/\mu\mathrm{m}$, and $E'_{\perp} = 1{\cdot}01\ \mathrm{V}/\mu\mathrm{m}$. For high field strength, the ratio r/R becomes 1 and the fingerprint pattern consists of straight lines perpendicular to the field. This behaviour indicates that the pitch axis **q** progresses from a radial structure ($E = 0$), to an axial structure ($E \approx E_0 + E'$), and finally to a uniform orientation of **q** along the field direction ($E \gg E_0 + E'$).

When the electric field is decreased and the director field relaxes from the high field configuration, it is possible to observe metastable states. If the droplet has not been completely reoriented, i.e. $r < R$, and the voltage is reduced slowly, the system remains in its equilibrium state and the growth and shrinking of the disclination ring is reversible with little hysteresis. However, if a very high voltage is rapidly reduced or suddenly switched off, the structure does not maintain its equilibrium state. In such a case, a metastable state can occur which is characterized by several stacked disclination rings parallel to, but not in, the equatorial plane (see figures 2 (*d*) and (*e*)). These rings then recombine successively in time to give one ring in the equatorial plane. This process is connected to the movement of the radial $s = 2$ disclination associated with the Frank–Pryce structure. Observations parallel to **E** indicate that this disclination line is oriented perpendicular to **E** and that it rotates around the field direction while r decreases gradually on each rotation [12]. In addition, our observations perpendicular to **E** shows that the trajectory of this disclination line is a spiral, i.e. while rotating about **E** it also moves along **E** thereby enabling the recombination of the disclination rings.

A second metastable state occurs after this recombination process (see figure 2 (*f*)). In contrast to the pattern on increasing voltage, in one hemisphere the fingerprint lines are parallel while in the other hemisphere their projections intersect in a complicated way, which makes it difficult for us to conclude their exact arrangement. In this

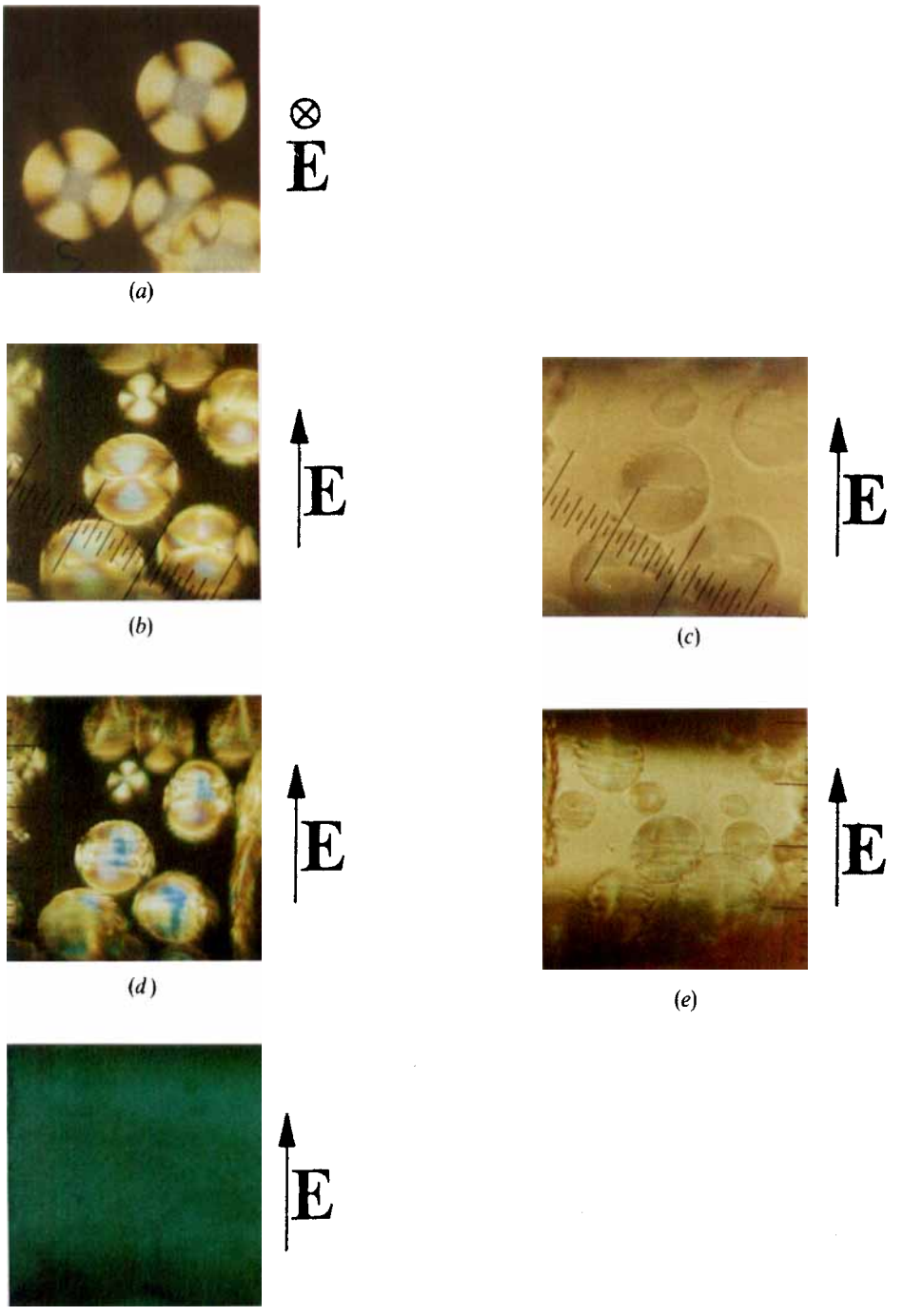

Figure 2. Microphotographs of cholesteric droplets with $\epsilon_a < 0$ under the influence of a 1 kHz electric field. (*a*) Composition 2·7 wt% CE2, 47·3 per cent ZLI 2806, 50·0 per cent PVB; $E = 0{\cdot}96\ \mathrm{V}/\mu\mathrm{m}$, observation $\|\mathbf{E}$, crossed polarizers. (*b*) Composition 2·9 wt% CE2, 46·9 per cent ZLI 2806, 50·2 per cent PVB; $E = 0{\cdot}69\ \mathrm{V}/\mu\mathrm{m}$, observation $\perp\mathbf{E}$, crossed polarizers. (*c*) Same parameters as in (*b*), but observation without polarizers. (*d*) Same sample as in (*b*), 1 s after switching off $2{\cdot}0\ \mathrm{V}/\mu\mathrm{m}$, crossed polarizers. (*e*) Same parameters as in (*d*), no polarizers. (*f*) Same sample as in (*b*), 10 s after switching off $2{\cdot}0\ \mathrm{V}/\mu\mathrm{m}$.

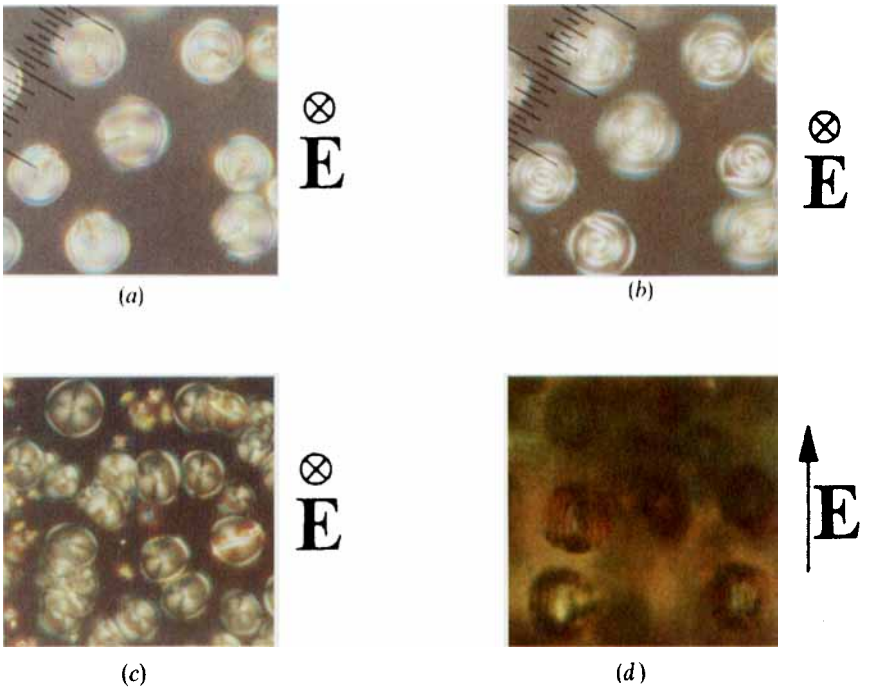

Figure 4. Microphotographs of cholesteric droplets with $\epsilon_a > 0$ under the influence of a 1 kHz electric field. Composition 4·4 wt% CB15, 45·4 per cent E9, 50·2 per cent PMMA. (*a*) $E = 0$. (*b*) $E = 1{\cdot}12\ \mathrm{V}/\mu\mathrm{m}$, observation $\|\mathbf{E}$. (*c*) $E = 1{\cdot}6\ \mathrm{V}/\mu\mathrm{m}$, observation $\|\mathbf{E}$. (*d*) $E = 1{\cdot}3\ \mathrm{V}/\mu\mathrm{m}$, observation $\perp\mathbf{E}$.

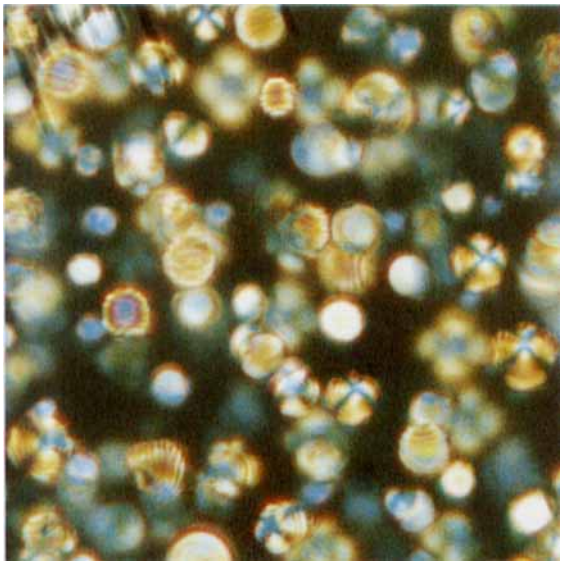

Figure 7. Microphotograph of cholesteric droplets with perpendicular anchoring (1·8 wt% CE2, 45·8 per cent EN18, 52·4 per cent PIBMA).

situation, the central disclination ring stops shrinking. Finally, as late as several minutes after removal of the voltage, the ring disappears due to a sudden discontinuous rearrangement within the entire hemisphere. The second metastable state is obviously identical to the metastable state reported in [12] which was also observed parallel to the field.

3.3. *Planar anchoring, $\epsilon_a > 0$*

In comparison with the observations described here, cholesteric droplets with $\epsilon_a > 0$ behave quite differently in electric fields. When observed parallel to the field direction, the distance between the fingerprint lines increases (see figures 4 (*a*) and (*b*)). Recalling that the distance between fingerprint lines corresponds to the half-pitch [10], this behaviour indicates an increase of p as is well-known for a cholesteric phase with $\epsilon_a > 0$ in the bulk [16]. In contrast to systems with $\epsilon_a < 0$, the field does not cause the appearance of an additional disclination line within the droplets. In the field, most droplets show the spiral type of pattern as represented in figure 1 (*b*), indicating that the radial $s = 2$ disclination line is preferentially oriented parallel to the field direction. Eventually, reorientation at small field strength causes a small textural change which has little influence on p. For higher fields, p increases, and above a threshold E_c the fingerprint lines disappear completely, indicating complete unwinding to the nematic state (see figure 4 (*c*)). For observation perpendicular to the field (see figure 4 (*d*)), the concentric fingerprint lines first take on an ellipse-like shape where, in contrast to $\epsilon_a < 0$, the long axes are oriented parallel to the field. The same texture has been observed previously for cholesteric droplets in a magnetic field perpendicular to the viewing direction [9]. For higher fields the fingerprint lines become parallel to **E** and finally vanish for $E > E_c$.

Measurements of the pitch versus field strength (see figure 5) indicate that the threshold field E_c depends on the intrinsic pitch p_0 at $E = 0$, as expected from the relation

$$E_c = (4\pi^2/p_0)(K_2/\epsilon_a)^{1/2}$$

which describes helical unwinding of the cholesteric phase in the bulk [16]. By variation of the chirality, we have found that E_c is indeed proportional to p_0^{-1} within our experimental accuracy (see figure 6).

When the field is reduced, the droplets show a remarkable hysteresis, i.e. the nematic texture characterized by the absence of fingerprint lines can be metastable for $E < E_c$. On decreasing voltage, the intensity of the maltese cross observed in the droplet centre (see figure 4 (*c*)) increases. Several volts below E_c, fingerprint lines start to reappear for some droplets. This reappearance is a discontinuous process changing the entire texture of a droplet. The distance between the fingerprint lines indicates that the pitch at this voltage is much smaller than the diameter of the respective droplet. Besides the relaxation of single droplets, there is a second threshold $E_{c,2}$, where most of the droplets return to the fingerprint texture all at once. Obviously the metastable nematic texture is unstable below $E_{c,2}$. Variation of the chirality shows that $E_{c,2}$ is also proportional to p_0^{-1} (see figure 6). For the systems investigated here, the ratio between the threshold voltages $E_{c,2}/E_c$ is about 0·55.

3.4. *Perpendicular anchoring*

Finally, we report on a new type of cholesteric droplet structure which is observed for perpendicular anchoring of the director at the droplet surface. Using PIBMA as the

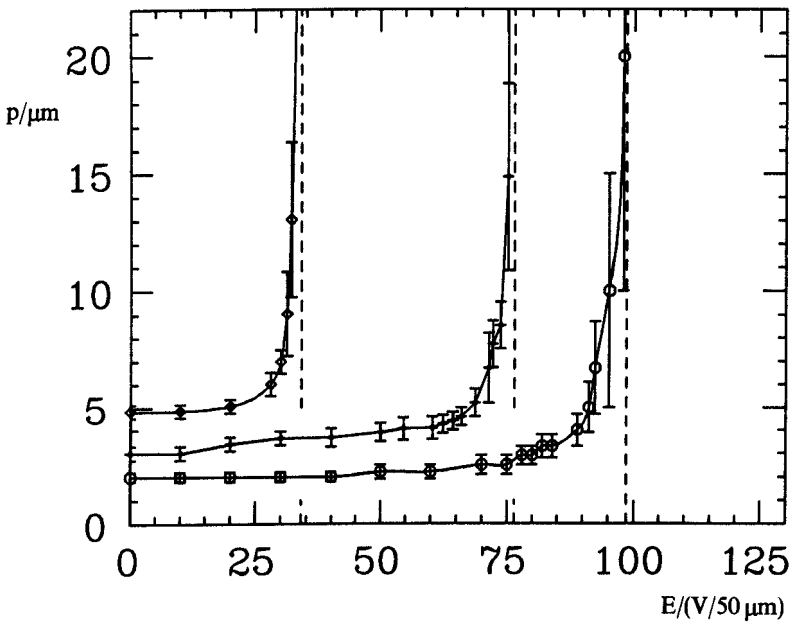

Figure 5. Pitch of cholesteric droplets with $\epsilon_a > 0$ versus field strength (same system as figure 4, but different concentrations of the chiral compound CB15).

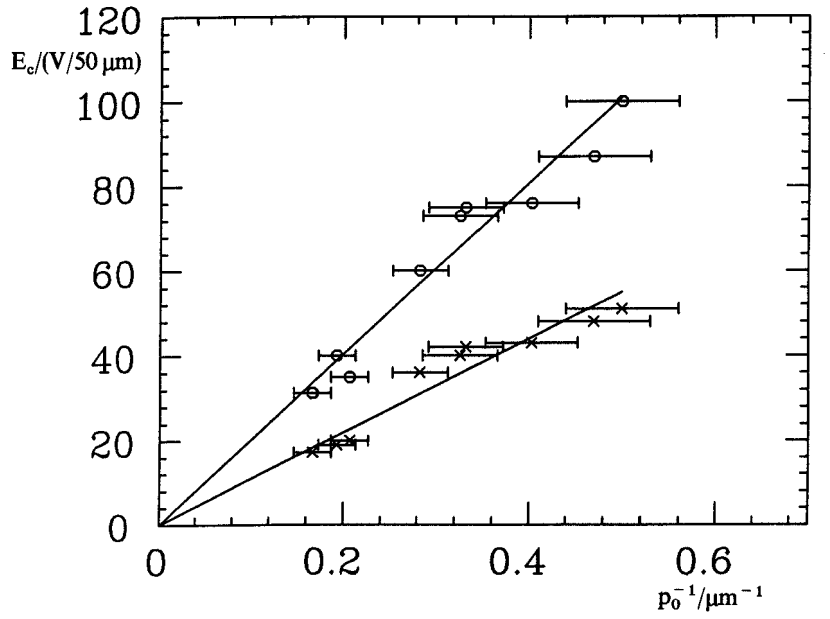

Figure 6. Threshold field strengths E_c (○) and $E_{c,2}$ (×) for cholesteric droplets with $\epsilon_a > 0$ versus reciprocal pitch.

polymer matrix, we observe fingerprint patterns whose appearance depends on the orientation of the droplet (see figure 7). For some droplets, the fingerprint lines are concentric as in the case of planar anchoring, but for other droplets they are elliptical and their centre does not coincide with the droplet centre. In addition, other droplets show parallel fingerprint lines. We conclude, that these different patterns correspond to the same director field but to different orientations of the droplet.

In general, surfaces with perpendicular anchoring for nematic phases are known to cause parallel orientation of the pitch axes **q** for a cholesteric. Recalling that the fingerprint lines observed in cholesteric phases are perpendicular to the helix axis, our observations are in agreement with a bipolar arrangement of the helix axes (see figure 8 (*k*)). In this case, we expect concentric fingerprint lines for observation along the axis connecting the two poles while almost parallel fingerprint lines are expected for observation perpendicular to the polar axis.

This model is confirmed by the effect of an electric field on a liquid crystal with $\epsilon_a < 0$ (CE2/EN18). Application of a voltage leads to the appearance of a Grandjean texture within the droplets as observed previously. After the voltage is removed the fingerprint lines reappear, but all of the droplets show concentric patterns for observation along the former field direction, independent of their previous texture. We conclude that the electric field has an orienting influence on the proposed bipolar structure. Preferential orientation of the polar axis parallel to the field is in good agreement with the preferred alignment of the director perpendicular to the field as expected for a liquid crystal with $\epsilon_a < 0$. However, more detailed studies on the behaviour of droplets with perpendicular surface anchoring in electric fields are in progress.

4. Conclusion: a classification scheme for chiral droplets

We have studied the behaviour of chiral nematic droplets with planar anchoring in electric fields applied both parallel and perpendicular to the direction of observation. Considering the direction of the pitch axes **q**(**r**) we note that there are some analogies with the director fields **n**(**r**) of non-chiral nematic droplets. We suggest, therefore, a classification of the structures of chiral droplets which is similar to the classification of structures of the well-investigated nematic droplets (see figure 8). For non-chiral nematic droplets, radial [15], axial [15], hyperbolic [17], and escaped structures [14] have been observed for perpendicular anchoring, while bipolar [15] and concentric structures [15] are known to occur for parallel anchoring (see figures 8 (*a*)–(*f*)). We postulate, therefore, that similar structures occur for the vector field **q**(**r**) of a chiral droplet, provided that the respective anchoring is just opposite to the analogous nematic structure (recall that **n** is perpendicular to **q** in a cholesteric helix). Thus the perpendicularly anchored nematic droplet with radial **n** is analogous to the parallel anchored chiral droplet with radial **q** as is indeed observed (see figure 8 (*g*)). However, the analogy between a radial nematic droplet and a radial cholesteric droplet does not extend to the type of induced defect. Radial nematic droplets show a disclination point at their centre while the Frank–Pryce model for chiral droplets is characterized by the occurrence of a radial disclination line.

Under the influence of electric fields, radial nematic droplets with $\epsilon_a > 0$ are known to transform to the axial structure [18]. In analogy, our chiral droplets with $\epsilon_a < 0$ show an axial vector field **q**(**r**) if a field is applied, since the pitch axis tends to align along the field direction for materials with $\epsilon_a < 0$ (see figure 8 (*h*)). Both the nematic axial structure **n**(**r**) and the cholesteric axial structure **q**(**r**) show a disclination ring perpendicular to the applied field. However, a discontinuous field-induced transition from a pure radial

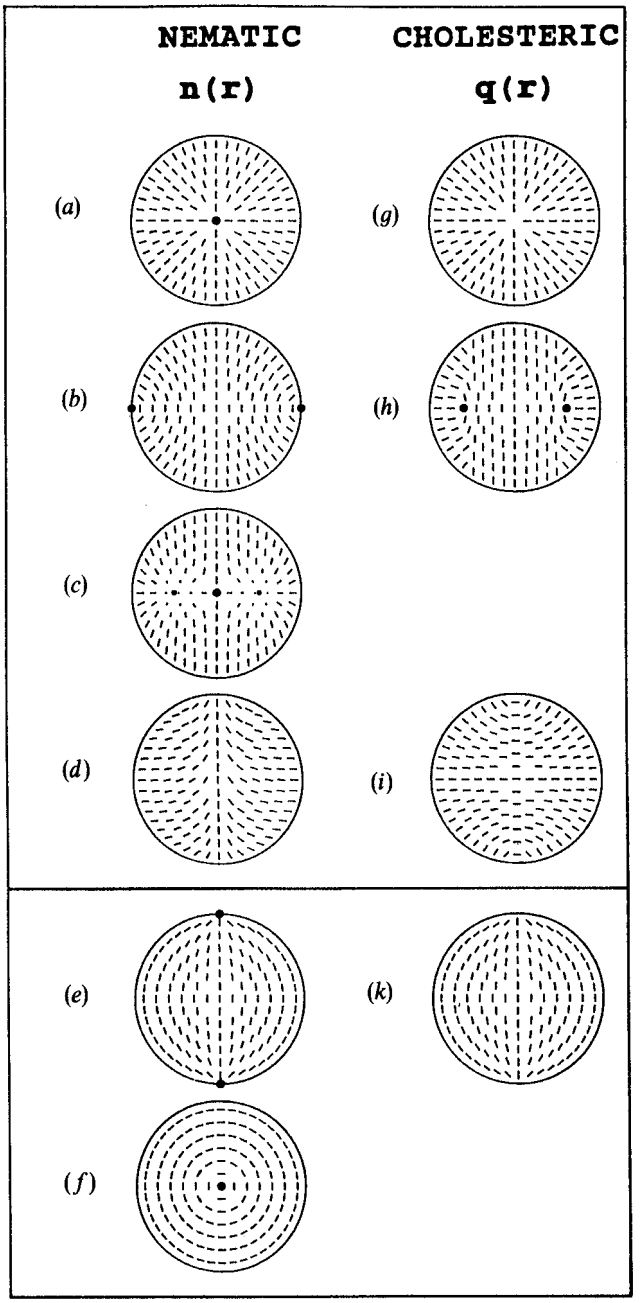

Figure 8. Structures of droplets. The nematic configurations (*a*)–(*f*) are represented by the director **n**(**r**) while for the cholesteric droplets (*g*)–(*k*) the pitch axis **q**(**r**) is given. (*a*) Radial, (*b*) axial, (*c*) hyperbolic, (*d*) escaped, (*e*) bipolar, (*f*) concentric, (*g*) Frank–Pryce model (planar anchoring), (*h*) planar anchoring, $\epsilon_a < 0$, $E \neq 0$, (*i*) planar anchoring, $\epsilon_a > 0$, $E \neq 0$, (*k*) perpendicular anchoring.

structure to an axial structure with an equatorial defect line was reported for nematic droplets [18]. In contrast, we found the disclination ring to grow continuously with increasing field strength (see figure 3) for cholesteric droplets.

For cholesteric liquid crystals with $\epsilon_a > 0$, we observe a different axial structure which is characterized by **q**(**r**) mainly perpendicular to the field direction (see figure 8 (*i*)). An analogous structure for nematic droplets which might be expected for nematic droplets with $\epsilon_a < 0$ has not yet been observed. Instead, an escaped director field has been found recently [14]. This different behaviour can be explained by the fact that a cholesteric axial structure with **q** perpendicular to the axis does not require a disclination; that is, the twist has effectively caused an escape along the diameter. An analogous director field **n**(**r**), however, would show a diametrical $s = 1$ disclination line along the central axis. In reality, such a structure also escapes along the diameter rather than supporting the diametrical defect [14]. For cholesteric droplets with perpendicular anchoring, our observations reveal a bipolar structure of the field **q**(**r**) (see figure 8 (*k*)), which is analogous to the director field of nematic droplets with planar anchoring. The influence of electric fields on cholesteric droplets with perpendicular boundary conditions has still to be investigated.

In conclusion, we have observed some new cholesteric structures and have attempted to classify them by analogy with previously observed nematic structures. These analogies are based solely on experimental observations; the intention is to classify the various cholesteric structures and perhaps to point the way to possible new director arrangements. We caution, however, that the analogies are not yet rigorous. To achieve such rigor, a more solid theoretical framework is required.

In particular, since a description of cholesteric structures requires not only the direction of **q** but also the phase of the respective Fourier component of the order parameter, there may be more than one possible director configuration for radial **q**(**r**) analogous to the radial **n**(**r**) field. Bezic and Žumer [19] have discussed several cholesteric droplet structures for parallel surface anchoring which all exhibit radial **q**(**r**). Because the phase of the twist axes differs between the structures, the topologies and especially the nature of the respective defects is quite different for each structure.

It is expected that new structures, both nematic and cholesteric, have yet to be observed. The stability of these structures is expected to depend on elastic constant ratios, anchoring strengths and anchoring direction, and size of the applied field, the full range of which have yet to be fully explored.

H.-S. K. would like to thank the Department of Physics and Astronomy, University of Hawaii, for their very kind hospitality. We thank J. W. Doane, J. L. West, and G. P. Crawford (Kent State University) for advice on obtaining perpendicular anchoring. This work was supported by the Office of Technology Transfer and Economic Development of the University of Hawaii and by the Deutsche Forschungsgemeinschaft (Sfb 335).

References

[1] Doane, J. W., Golemme, A., West, J. L., Whitehead, J. B., and Wu, B.-G., 1988, *Molec. Crystals liq. Crystals*, **165**, 511.

[2] Doane, J. W., 1990, *Liquid Crystals—Applications and Uses*, Vol. 1, edited by B. Bahadur (World Scientific Publishing Company), pp. 361–395.

[3] Crooker, P. P., and Yang, D. K., 1990, *Appl. Phys. Lett.*, **57**, 2529.

[4] Kitzerow, H.-S., Molsen, H., and Heppke, G., 1992, *Appl. Phys. Lett.*, **60**, 3093.

[5] LEHMANN, O., 1908, *Flüssige Kristalle und die Theorien des Lebens* (Verlag Johann Ambrosius Barth).
[6] FRIEDEL, G., 1922, *Annls. Phys.*, Série 9, **18,** 273.
[7] ROBINSON, C., WARD, J. C., and BEEVERS, R. B., 1958, *Discuss. Faraday Soc.*, **25,** 29.
[8] ROBINSON, C., 1966, *Mole. Crystals*, **1,** 467.
[9] CANDAU, S., LE ROY, P., and DEBEAUVAIS, F., 1973, *Molec. Crystals liq. Crystals*, **23,** 283.
[10] BOULIGAND, Y., and LIVOLANT, F., 1984, *J. Phys. France*, **45,** 1899.
[11] YANG, D. K., and CROOKER, P. P., 1990, *Liq. Crystals*, **9,** 245.
[12] KITZEROW, H.-S., and CROOKER, P. P., 1992, *Liq. Crystals*, **11,** 561.
[13] SHURCLIFF, W. A., 1962, *Polarized Light* (Harvard University Press).
[14] XU, F., KITZEROW, H.-S., and CROOKER, P. P., 1992, *Phys. Rev.* A (in the press).
[15] ONDRIS-CRAWFORD, R., BOYKO, E. P., WAGNER, B. G., ERDMANN, J. H., ŽUMER, S., and DOANE, J. W., 1991, *J. appl. Phys.*, **69,** 6380.
[16] DE GENNES, P. G., 1968, *Solid St. Commun.*, **6,** 163.
[17] LAVRENTOVICH, O. D., and TERENT'EV, E. M., 1986, *Sov. Phys. JETP*, **64,** 1237.
[18] ERDMANN, J. H., ŽUMER, S., and DOANE, J. W., 1990, *Phys. Rev. Lett.*, **64,** 1907.
[19] BEZIC, J., and ŽUMER, S., 1992, *Liq. Crystals*, **11,** 593.